Molecular Cell, Vol. 9, 1227–1240, June, 2002, Copyright ©2002 by Cell Press

Molecular Mechanism for the Regulation of Protein Kinase B/Akt by Hydrophobic Motif Phosphorylation

Jing Yang,[1] Peter Cron,[2] Vivienne Thompson,[1] Valerie M. Good,[1] Daniel Hess,[2] Brian A. Hemmings,[2,3] and David Barford[1,3]
[1]Section of Structural Biology
Institute of Cancer Research
Chester Beatty Laboratories
237 Fulham Road
London, SW3 6JB
United Kingdom
[2]Friedrich Miescher-Institut
Maulbeerstrasse 66
CH-4048, Basel
Switzerland

Summary

Protein kinase B/Akt plays crucial roles in promoting cell survival and mediating insulin responses. The enzyme is stimulated by phosphorylation at two regulatory sites: Thr 309 of the activation segment and Ser 474 of the hydrophobic motif, a conserved feature of many AGC kinases. Analysis of the crystal structures of the unphosphorylated and Thr 309 phosphorylated states of the PKB kinase domain provides a molecular explanation for regulation by Ser 474 phosphorylation. Activation by Ser 474 phosphorylation occurs via a disorder to order transition of the αC helix with concomitant restructuring of the activation segment and reconfiguration of the kinase bilobal structure. These conformational changes are mediated by a phosphorylation-promoted interaction of the hydrophobic motif with a channel on the N-terminal lobe induced by the ordered αC helix and are mimicked by peptides corresponding to the hydrophobic motif of PKB and potently by the hydrophobic motif of PRK2.

Introduction

The serine/threonine protein kinase PKB/Akt is a critical component of an intracellular signaling pathway that exerts the effects of growth and survival factors and that mediates the response to insulin and inflammatory agents (Datta et al., 1999; Brazil and Hemmings, 2001). PKB is activated as a consequence of agonist-induced stimulation of PI3 kinase and generation of the phospholipid PtdIns(3,4,5)P_3. This second messenger interacts with the PH domain of PKB, recruiting the kinase to the plasma membrane and exposing a pair of serine and threonine residues for phosphorylation by membrane-associated protein kinases. PDK1 phosphorylates PKB on a Thr residue (Thr 309 of PKBβ) of the activation segment. The unphosphorylated form of PKB is virtually inactive, and PDK1 phosphorylation stimulates its activity by at least 100-fold (Alessi et al., 1996, 1997; Stokoe et al., 1997; Stephens et al., 1998). A distinct kinase activity, termed PDK2, phosphorylates PKB at Ser 474 of its C-terminal hydrophobic motif. Phosphorylation of Ser 474 augments the activity of PDK1-phosphorylated PKB by 7- to 10-fold (Alessi et al., 1996), such that phosphorylation of both residues results in greater than 1000-fold increased protein kinase activity.

PKB is responsible for phosphorylating numerous nuclear and cytosolic proteins that regulate cell metabolism and growth. For example, during insulin signaling, the kinase phosphorylates GSK-3, PFK2, and mTOR to induce glycogenesis and protein synthesis, while the phosphorylation of proteins that regulate apoptosis such as BAD, caspase-9, forkhead transcription factors, and IκB kinase promotes proliferation and survival (Datta et al., 1999). PKB stimulates cell cycle progression by phosphorylation of the CDK inhibitors $p21^{WAF1}$ and $p27^{Kip1}$, causing their retention in the cytoplasm, whereas mdm2 is localized to the nucleus to suppress p53 (Mayo and Donner, 2001). PKB plays an important role in the generation of human malignancy. The enzyme is the cellular homolog of *v*-Akt, an oncogene of the transforming murine leukaemia virus AKT8 isolated from a mouse lymphoma (Staal et al., 1977). Viral-Akt is a fusion of the viral Gag protein with the PKBα sequence (Bellacosa et al., 1991). Myristoylation of the Gag sequence targets *v*-Akt to the cell membrane, resulting in its constitutive phosphorylation. The genes for the α and β isoforms of PKB are overexpressed and amplified in ovarian, prostate, pancreatic, gastric, and breast tumors (Testa and Bellacosa, 2001). Moreover, the finding that *PTEN*, one of the most commonly mutated genes in human cancer, encodes a PtdIns(3,4,5)P_3 lipid phosphatase, provided compelling evidence linking PKB to oncogenesis (Cantley and Neel, 1999).

In humans, the three isoforms of PKB are highly conserved, sharing the same regulatory phosphorylation sites. However, a splice variant of PKBγ lacks the C-terminal regulatory phosphorylation site, and interestingly the specific activity of this splice variant, isolated from stimulated cells, is ~10-fold lower than the full-length γ isoform, a value that is consistent with the role of the C-terminal phosphorylation site to stimulate PKB activity (Brodbeck et al., 2001). CTMP is a negative regulator of PKB, which by binding to the C-terminal region of the protein suppresses phosphorylation of Thr 309 and Ser 474 (Maira et al., 2001).

Protein kinase B is a member of the AGC family of protein kinases that includes PKA, PKC, PDK1, and the p70 and p90 S6 kinases (Coffer and Woodgett, 1991; Jones et al., 1991a). As well as being structurally related, AGC-protein kinases share numerous functional similarities such as activation in response to second messengers and dependence on phosphorylation for activity. Members of the family are phosphorylated on a conserved Thr residue within their activation segment. In vitro PDK1 is capable of phosphorylating AGC kinases on this position (Vanhaesebroeck and Alessi, 2000), although recent studies using PDK1-deficient ES cells suggest that PDK1 activity is only necessary for PKB and a subset of other AGC kinases (Williams et al., 2000).

[3]Correspondence: dbarford@icr.ac.uk (D.B.), hemmings@fmi.ch (B.A.H.)

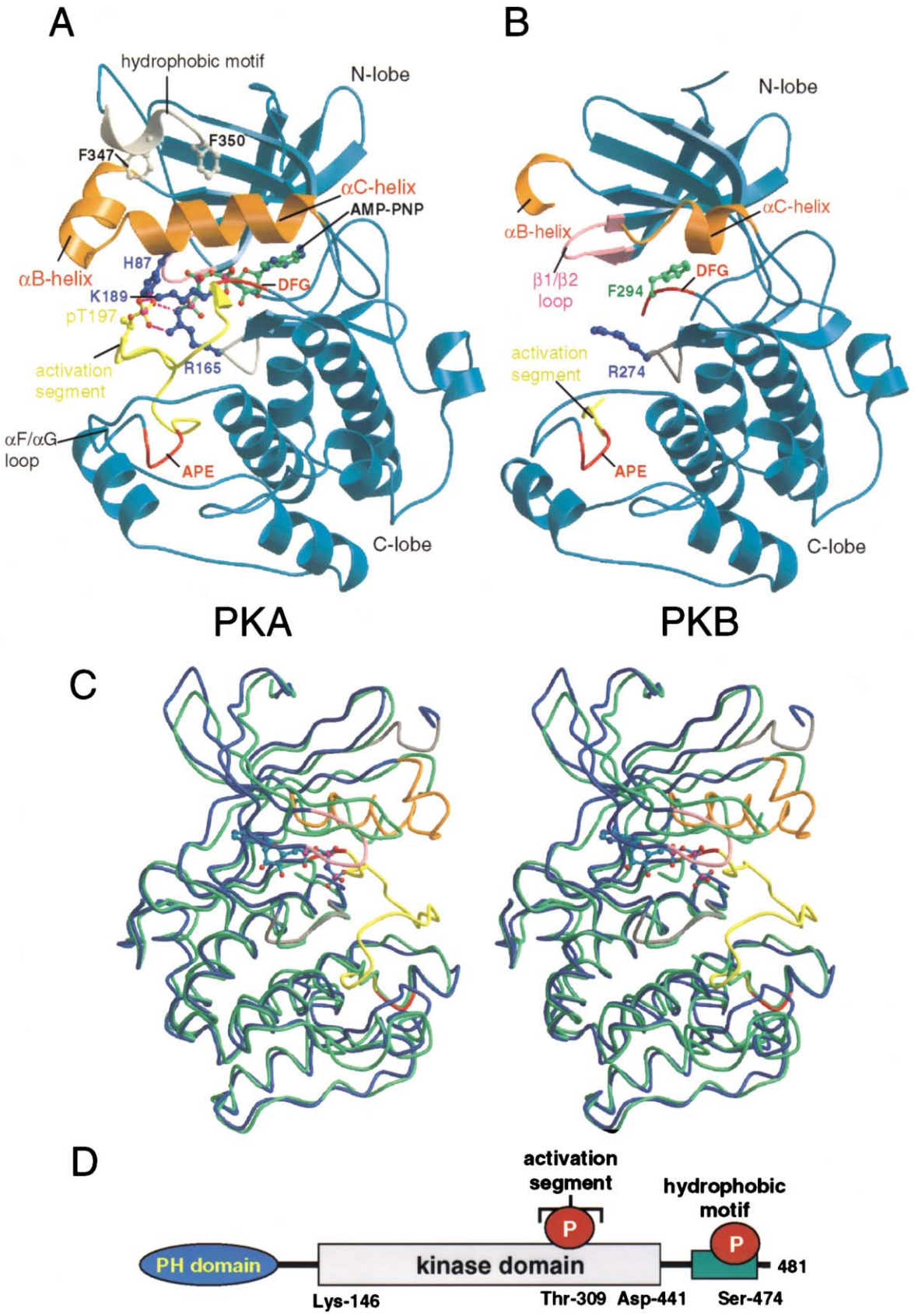
A
hydrophobic motif
N-lobe
F347
F350
αC-helix
AMP-PNP
αB-helix
H87
DFG
K189
pT197
activation segment
R165
αF/αG loop
APE
C-lobe
PKA
B
N-lobe
αC-helix
αB-helix
β1/β2 loop
F294
DFG
activation segment
R274
APE
C-lobe
PKB
C
D
activation segment
hydrophobic motif
P
P
PH domain
kinase domain
481
Lys-146
Thr-309
Asp-441
Ser-474

The site of C-terminal regulatory phosphorylation of PKB (Ser 474) is within a hydrophobic sequence motif (F-x-x-F-[S/T]-Y), conserved within a large proportion of AGC kinases (Keranen et al., 1995; Pearson et al., 1995). In PKB, substitution of Asp for Ser 474 mimics Ser 474 phosphorylation (Alessi et al., 1996), and significantly some atypical PKC isoforms and PRK2 (PKC related kinase 2) have Asp or Glu residues at this position. PKA requires phosphorylation of the activation segment Thr residue (Thr 197) for activity (Yonemoto et al., 1997), although this is a constitutive site of phosphorylation, and unlike other AGC kinases is resistant to dephosphorylation by protein phosphatases (Shoji et al., 1979). The hydrophobic motif of PKA is also unusual and comprises the sequence -Phe-Thr-Glu-Phe-350, with Phe 350 corresponding to the C terminus of the PKA catalytic subunit, and therefore the enzyme lacks a site of regulatory phosphorylation.

Here we describe crystallographic, thermodynamic, and kinetic studies of the kinase, revealing the molecular basis of regulation by hydrophobic motif phosphorylation. Activation of PKB by Ser 474 phosphorylation occurs via a mechanism involving a disorder to order transition of the αC helix of the N-terminal lobe, induced by the association of a phosphorylated hydrophobic motif, with concomitant ordering and restructuring of the activation segment and alignment of catalytic site residues.

Results and Discussion

Structure Determination

Crystals of the kinase domain of the β isoform of human PKB were obtained by delineating a protease-resistant, structurally compact domain and by controlling the phosphorylation state of the protein in vitro. We expressed two forms of PKB in *Sf*9 cells with an N terminus following the preceding PH domain and linker region (Figure 1). One form, ΔPH-PKB-ΔC, corresponds to the minimum kinase domain without the C-terminal 21 residues that contain the hydrophobic motif (HM) including Ser 474, whereas the second form, ΔPH-PKB, contains the hydrophobic motif. To prepare defined phosphorylated states of these proteins, phosphorylation and dephosphorylation reactions were performed using PDK1 (for pThr 309) and the nonspecific λ protein phosphatase, respectively. The phosphorylation states of the proteins were analyzed by Western blots using phosphospecific antibodies, and the stoichiometry and sites of phosphorylation were quantitatively assessed by mass spectroscopic analysis. Only the β isoform crystallized, and we obtained three crystal forms that differ in their state of phosphorylation and by the presence of the hydrophobic motif: (1) pΔPH-PKB-ΔC, phosphorylated in vitro on Thr 309, (2) ΔPH-PKB-ΔC, not phosphorylated on Thr 309, and (3) ΔPH-PKB, dephosphorylated in vitro (Table 1). These three crystal forms are isomorphous and diffract up to 2.3 Å resolution when exposed to synchrotron radiation (Table 1). Solution of the structure was by means of molecular replacement using the ternary complex of mouse PKA (Knighton et al., 1991) (Table 1).

Overall Structure of PKB and Comparison with PKA

The structure of pΔPH-PKB-ΔC is essentially identical to those of ΔPH-PKB-ΔC and ΔPH-PKB (rms deviations of 0.3 and 0.4 Å, respectively), and this similarity to inactive forms of PKB, together with features of the structure, indicates that the crystallization conditions favored the inactive conformation of pΔPH-PKB-ΔC. Our discussion is focused on the pΔPH-PKB-ΔC crystal structure because of its higher resolution.

As expected, the overall structure of pΔPH-PKB-ΔC resembles that of the related catalytic subunit of PKA (Figure 1). The two protein kinases share essentially the same secondary structure topology, except that in PKB there is no counterpart to the αA helix of PKA, and some of the structural elements of PKB are disordered. The architecture of PKA consists of an N-terminal lobe based on a five-stranded β sheet, with two α helices (the αB and αC helices), and a larger, mainly α-helical C-terminal lobe, containing the activation segment. The catalytic site for ATP is located at the interface of the two lobes, and the substrate peptide binding site is within the C lobe, centered on the activation segment. The inactive state of PKB differs in structure from the catalytically active form of PKA in a number of respects that are important for the regulation of PKB by multisite phosphorylation. These differences involve the overall juxtaposition of the N and C lobes of the kinase and structural disorder of the αB and αC helices of the N lobe, activation segment of the C lobe, and C-terminal regulatory segment. Compared with the PKA-ternary complex, the N lobe of PKB is rotated by 20° relative to its C lobe, causing catalytic site residues from the two lobes to be misaligned. When superimposed individually, differences in conformation between the equivalent N and C lobes of PKA and PKB are observed localized to the β1 strand and αC helix in the N lobe and DFG motif and αF/αG loop in the C lobe.

Structure of the N Lobe and Flexibility of the αB and αC Helices

Within the N-terminal lobe of PKB, the β sheet is well ordered; however, residues Ala 189 to Thr 207, equivalent to the αB helix and the majority of the αC helix of PKA, are highly mobile, as judged by disorder in the

Figure 1. Structure of PKB and Comparison with PKA

Ribbons representation of PKA (A) and PKB (B). Catalytic and regulatory structural elements are color coded, with αB and αC helices gold, DFG and APE motifs of the activation segment red, remainder of activation segment yellow, catalytic loop gray, β1/β2 glycine-rich loop pink, and hydrophobic motif of PKA gray. PKA and PKB were superimposed onto their C-terminal lobes. Phe 294 of the DFG motif of PKB occupies a site equivalent to the adenine pocket of the nucleotide binding site of PKA. (C) Stereo view of a superimposition of PKA and PKB to show different relative orientations of their N- and C-terminal lobes. Main chain coil of PKA is colored as in (A). PKB is colored green. Conformational differences in C lobe are localized to the activation segment and αF/αG loop. (D) Schematic of PKB. Figure drawn using BOBSCRIPT (Esnouf, 1997) and RASTER3D (Merit and Murphy, 1994)

Table 1. Crystallographic Data Collection and Refinement Statistics

Protein	pΔPH-PKBβ-ΔC	ΔPH-PKBβ-ΔC	ΔPH-PKBβ
Amino acid residues	146–460	146–460	146–481
Phosphorylation	Thr 309	–	–
Space group (Z)	$P4_12_12$ (1)	$P4_12_12$ (1)	$P4_12_12$ (1)
Cell parameters a (Å)	148.40	149.70	149.52
c (Å)	38.55	39.19	39.06
X-ray source	ID14eh4 ESRF	ID14eh4 ESRF	ID14eh4 ESRF
Resolution (Å)	2.3	2.7	2.5
Observations (N)	113 677	50 875	92 809
Unique (N)	18 905	12 147	16 090
Completeness (%)	96.1 (77.8)	94.2 (84.0)	99.7 (99.3)
[a]R_{sym}	0.050 (0.243)	0.065 (0.236)	0.057 (0.255)
I/σI	21.0	18.0	14.8
Refinement			
Resolution range (Å)	35–2.3	35–2.75	35–2.6
Reflections used (N)	17 576	10 320	14 317
R_{free} set (N) (%)	1 398 (7.1)	1 199 (9.9)	1 598 (10.0)
[b]R_{cryst}/R_{free}	0.237/0.309	0.238/0.30	0.254/0.314
Protein atoms (N)	2 198	2 198	2 198
Solvent atoms (N)	154	27	125
r.m.s.d. bond angles (°)	1.54	1.57	1.53
r.m.s.d. bond lengths (Å)	0.0105	0.0112	0.0104

Values in parentheses are for the highest shell.
[a]$R_{sym} = \Sigma_h\Sigma_j|<I(h)> - I(h)_j|/\Sigma_h\Sigma_j<I(h)>$, where $<I(h)>$ is the mean intensity of symmetry-equivalent reflections.
[b]$R_{cryst/free} = \Sigma||F_{obs}| - |F_{calc}||/\Sigma|F_{obs}|$, where F_{obs} and F_{calc} are the observed and calculated structure factors, respectively.
Root-mean-square deviations relate to the Engh and Huber parameters.

weighted 2Fo-Fc electron density, composite simulated annealing omit maps, and analysis of the atomic temperature factors (Figure 2A). Specifically, for all crystal forms, there is no visible electron density to account for residues Ala 189 to Thr 197, whose counterparts in PKA form the C terminus and N terminus of the αB and αC helices, respectively. The short αB helix, which connects the αC helix with the central β3 strand of the β sheet, is unique to the AGC-protein kinases and in PKA causes the N terminus of the αC helix to be displaced from the β4/β5 strands of the β sheet, creating a deep hydrophobic groove. In PKA this groove is responsible for interactions between the N-terminal lobe and C-terminal hydrophobic motif (Figures 1A and 2A).

The αC helix of the N lobe fulfils crucial catalytic and regulatory functions in all protein kinases. First, an invariant glutamate residue at the N terminus of the helix (Glu 91 of PKA, Glu 200 of PKB) contributes to its catalytic function by accepting a hydrogen bond from an invariant lysine side chain, Lys 72 of PKA (Figure 3). Lys 72 in turn coordinates the β phosphate of ATP in active protein kinases. Second, the αC helix is responsible for governing the overall juxtaposition of the N and C lobes by virtue of its extensive interfacial contacts with the C lobe, particularly via interactions with the DFG motif of the activation segment. Significantly, in many protein kinases that are regulated by phosphorylation of the activation segment, the αC helix provides a basic residue to contact the phospho-amino acid. In PKA, His 87 of the αC helix contacts pThr 197 (Figures 2B and 3A). In the inactive state of PKB, His 196 and Glu 200 of the αC helix (His 87 and Glu 91 of PKA) are disordered, and contacts between Glu 200 and Lys 181 (Lys 72 of PKA), and those between His 196 and pThr 309, are not formed (Figures 2C and 3B). Disorder of the αC helix contributes to an inactive state of PKB because the side chain of Lys 181 is not properly positioned, and there are associated changes in the structure of the activation segment and relative disposition of the N- and C-terminal lobes. As described below, disorder of the αB and αC helices of PKB is linked to the disorder of its nonphosphorylated C-terminal regulatory segment.

The C-Terminal Hydrophobic Motif Regulatory Segment

In PKA, residues of the hydrophobic motif interact with the hydrophobic groove of the N lobe (Figures 1A, 2B, and 4). These interactions are dominated by the side chains of Phe 347 and Phe 350, which protrude into the groove. Specifically, the phenyl ring of Phe 347 is extensively buried by the side chains of five amino acids: Lys 76, Val 79, and Val 80 of the αB helix, Ile 85 of the αC helix, and Leu 116 of the β5 strand, whereas the side chain of Phe 350 contacts Leu 89 and Lys 92 of the αC helix and Leu 116 and Met 118 of the β5 strand (Figure 2B). At one end of the channel, two adjacent basic residues of the αC helix (Lys 92 and Arg 93) form salt-bridge interactions with two carboxylate groups of the hydrophobic motif. In contrast to PKA, the crystal structures of PKB show that residues corresponding to the regions of the αB and αC helices, which in PKA interact with the hydrophobic motif, are disordered (Figure 2). This disorder probably results from loss of interactions with the hydrophobic motif of PKB. In the crystal structures of ΔPH-PKB-ΔC, the 21 residues C-terminal to Ser 460 were removed from the expression construct, and therefore potential interactions between the hydrophobic motif and the N lobe are not possible. Moreover, in these structures, electron density for residues C-terminal to Asp 441 is not visible, suggesting that they are conformational disordered. However, in the ΔPH-PKB structure, which contains a nonphosphorylated hy-

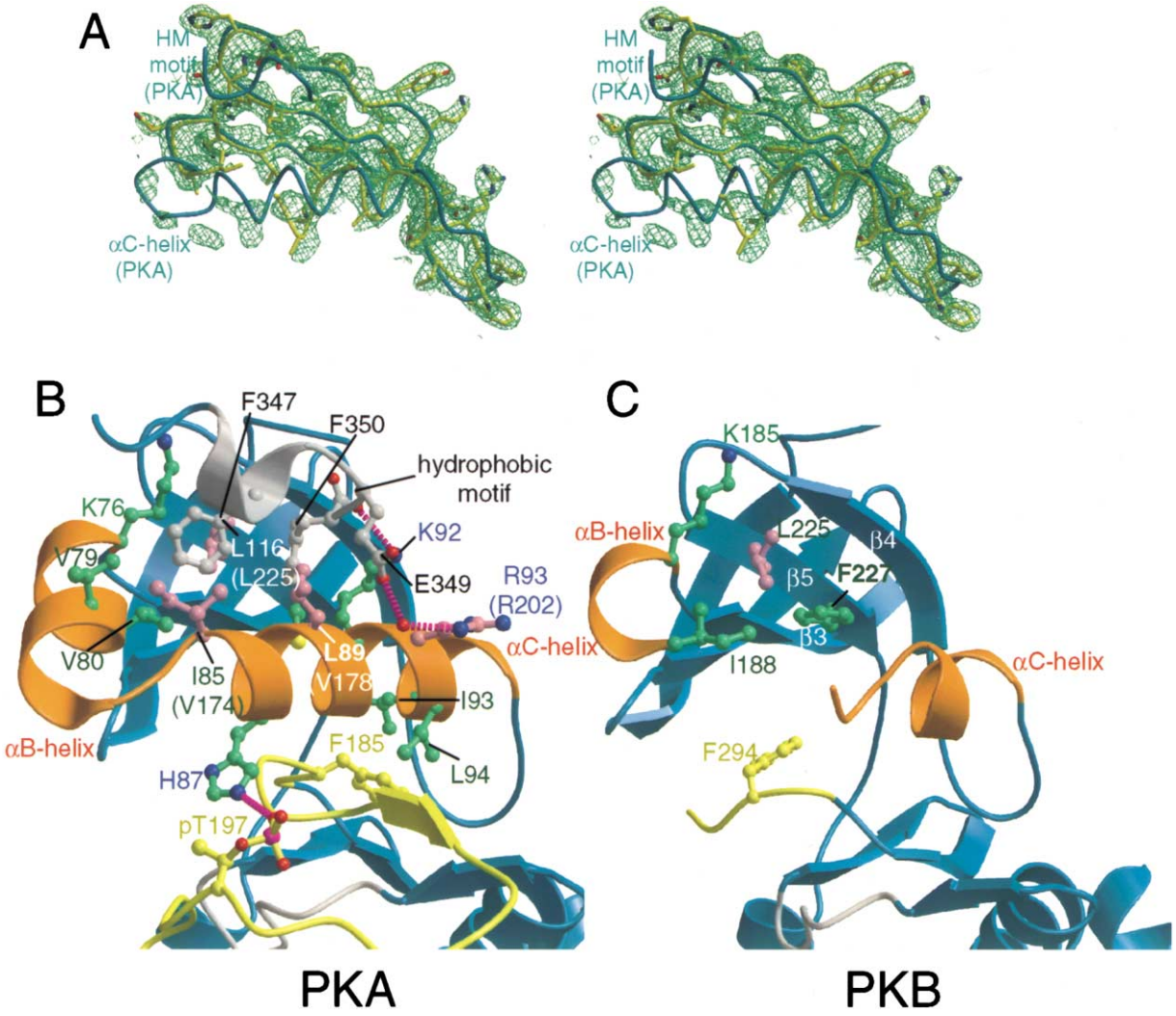

Figure 2. Structure of the N-Terminal Lobe

(A) Flexibility of αB and αC helices. 2Fo-Fc electron density map contoured at 1σ of a portion of the N-terminal lobe of pΔPH-PKB-ΔC (β3, β4, β5 strands, αB and αC helices). Electron density for the β sheet is well resolved, whereas the αB and αC helices are disordered. Main chain and side chain of PKB residues are shown as coil in yellow and atom bonds, respectively. The main chain of the N-terminal lobe and hydrophobic motif of PKA is shown in blue and superimposed onto PKB.

(B and C) Role of hydrophobic motif to order the αB and αC helices and link to activation segment. (B) Interactions of hydrophobic motif of PKA with the β5 strand and αB and αC helices of the N-terminal lobe. Phe 347 and Phe 350 are buried by hydrophobic residues. Glu 349 and C-terminal carboxylate form hydrogen bonds with basic residues of the αC helix. (C) Disorder of the αB and αC helices of PKB is correlated with absence of bound hydrophobic motif. Residues mutated to test responsiveness to PIFtide (Figure 7B) are colored pink. In (B) bracketed residues correspond to PKB numbering

drophobic motif and therefore retains the potential to interact with the N lobe, we are also unable to detect visible electron density for residues C-terminal to Asp 441, indicating that the hydrophobic motif is mobile.

Conformation of the Activation Segment and Nucleotide Binding Site

The activation segment is central to the regulation and catalytic activity of protein kinases (Johnson et al., 1996). In all three crystal forms of PKB, a contiguous region of the activation segment (residues 297 to 312) located between the invariant DFG and APE motifs, and including (p)Thr 309, is disordered. There is no electron density visible for these residues in either the 2Fo-Fc or the simulated annealing omit maps. In the inactive PKB structures, the ordered DFG motif adopts a different conformation from its counterpart in PKA, functioning to inhibit PKB by disrupting the nucleotide binding site (Figure 3). The Asp residue of the DFG motif of activated protein kinases is responsible for coordinating the Mg^{2+} ion of the ATP binding site. In PKB, the side chain of Asp 293 (equivalent to Asp 184 of PKA DFG motif) is directed away from the ATP binding site (Figure 3B). This structural change is accompanied by a shift in the positions of Phe 294 and Gly 295 of the DFG motif, and main chain of Leu 296, toward the glycine-rich β1-β2 nucleotide binding loop of the N lobe. Relative to the conformation of the equivalent Phe 185 residue of PKA,

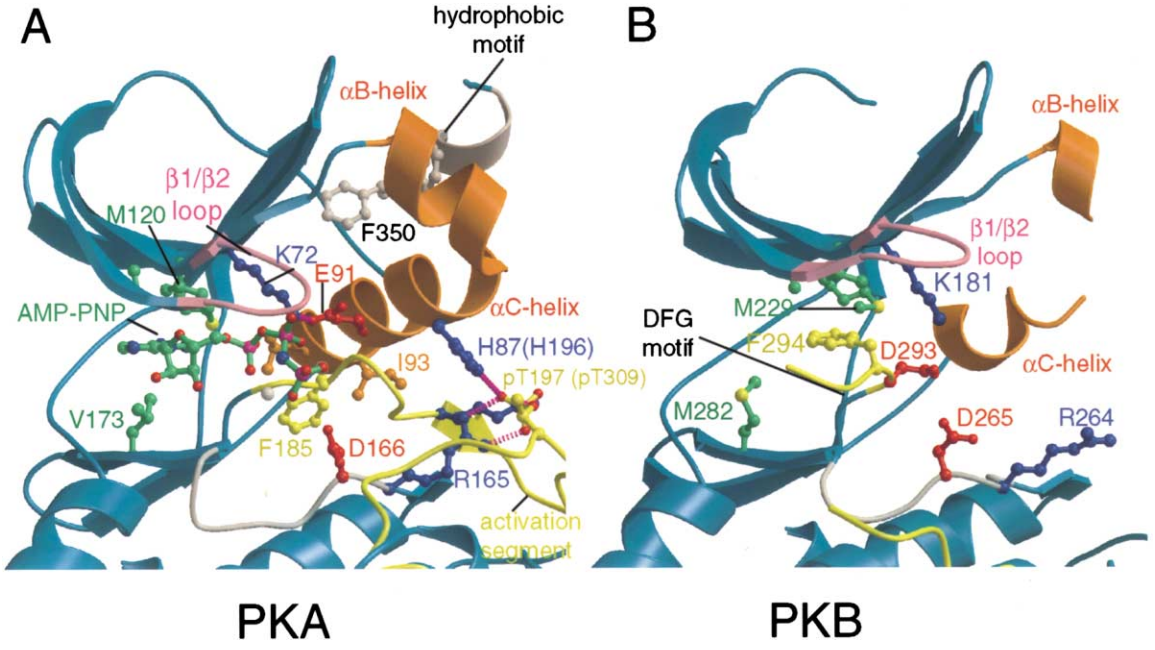

Figure 3. Role of αC Helix to Regulate Conformation of PKA and PKB and Structure of Activation Segment and DFG Motif

(A) αC helix stabilizes an active state of PKA by interaction with pThr 197 of the activation segment via His 87, and Phe 185 of the DFG motif via Ile 93 and Leu 94.

(B) In PKB, disorder of the αC helix prevents His 196 from interacting with pThr 309; Phe 294 of the DFG motif binds within the nucleotide binding site of ATP.

the phenyl ring of Phe 294 is displaced by 10 Å and forms hydrophobic contacts with the adenine binding pocket, a structural feature that was first observed in the inactive state of IRK (Hubbard et al., 1994). Thus, in PKB, the ATP binding site is disrupted both because Lys 181 and Asp 293, residues responsible for coordinating the phosphate groups, are displaced, and because ATP is sterically hindered from binding by Phe 294. Consequently, AMP-PNP/Mg^{2+} at 5 mM did not bind to the protein in the crystals. In PKA, the intimate contacts between Phe 185 of the DFG motif and hydrophobic residues of the αC helix stabilize the relative positions of the helix and activation segment. The altered conformation of Phe 294 of PKB is correlated with the relative dispositions of its N and C lobes and the disorder of the αC helix. Finally, disorder of the activation segment of PKB in both the unphosphorylated and monophosphorylated (pThr 309) states precludes interactions with protein substrates.

Mechanism of PKB Activation by Phosphorylation

PKB monophosphorylated on Thr 309 is ~10% as active as the fully phosphorylated enzyme. This implies that the conformational transition of PKB by multisite phosphorylation is allosteric: the enzyme exists in equilibria between inactive and active states, with the active state being promoted by the additive phosphorylation of Thr 309 and Ser 474. Only 10% of a population of PKB molecules monophosphorylated on Thr 309 will adopt an active conformation, and this explains why the crystal structure of PKB, monophosphorylated on Thr 309, adopts the same conformation as the inactive, unphosphorylated state of PKB. Under the conditions used for crystallization, the inactive conformer of the protein was selected in the crystal lattice. Additional Ser 474 phosphorylation stabilizes the active state, allowing most, and probably all, PKB molecules to adopt an active conformation.

Comparison with PKA explains how the inactive states of PKB lack catalytic activity and suggests that conversion to the activated state occurs by concerted reordering of the αB and αC helices, activation segment, and C-terminal regulatory segment, in a process linked to conformational changes of the DFG motif and reorientation of the N and C lobes. These changes would result in a kinase conformation similar to that of PKA phosphorylated on Thr 197. The three basic residues that coordinate pThr 197 of PKA are invariant in PKB, suggesting that pThr 197 and pThr 309 fulfil similar roles in the two kinases. However, PKB differs from PKA by its requirement for hydrophobic motif phosphorylation to achieve maximum kinase activity. In the PKA crystal structure, the hydrophobic motif lies within a hydrophobic groove formed by residues whose counterparts in the αB and αC helices of the inactive states of PKB are disordered. The unphosphorylated hydrophobic motif of ΔPH-PKB was disordered, suggesting that activation by Ser 474 phosphorylation is linked to the concomitant ordering of the hydrophobic motif and αB and αC helices mediated by the association of the motif with the induced N lobe hydrophobic groove. Ordering of the αC helix will induce global changes in the PKB conformation by facilitating interactions between the residues of the αC helix and critical regions of the molecule. These interactions include those between Lys 181 and Glu 200, and two αC helix-activation segment interactions, His

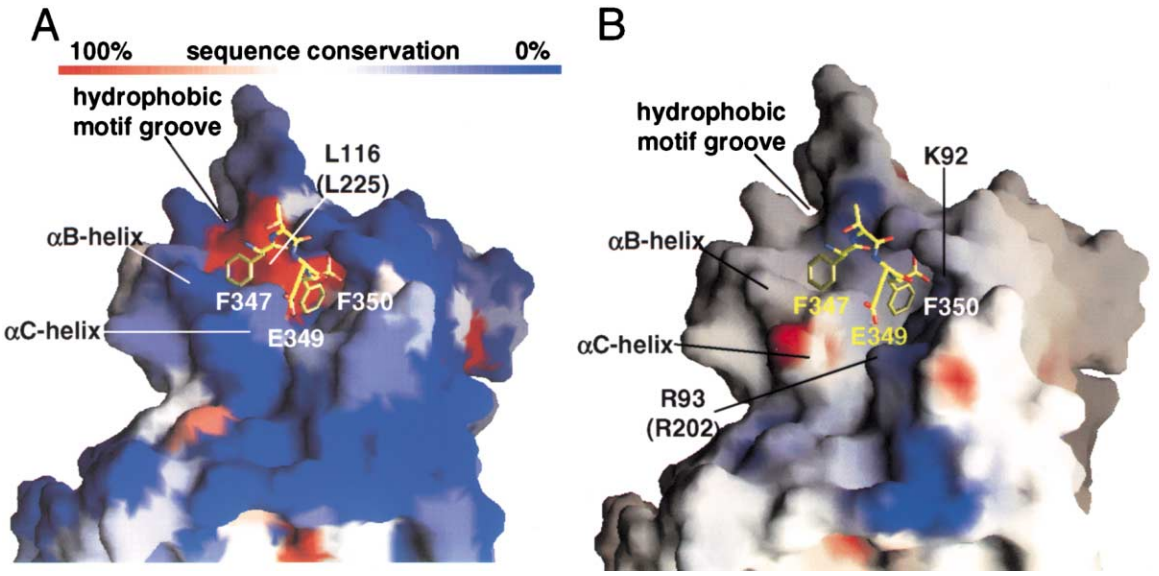

Figure 4. Features of the Hydrophobic Groove

(A) Conservation of hydrophobic motif binding channel among AGC kinases. The molecular surface of PKA is calculated with residues 340-350 omitted and is color coded according to sequence conservation with color ramped from red (invariant) to blue (nonconserved). Kinase sequences used to determine conservation are PKBβ, PKA, PKC, p70-S6K, p90-S6K, PDK1, SGK, and NDR1. Residues of the hydrophobic motif (Phe 347 to Phe 350) of PKA are shown. Figure drawn using GRASP (Nicholls et al., 1991).

(B) Electrostatic potential of the hydrophobic groove.

196 and pThr 309, and hydrophobic contacts with Phe 294 of the DFG motif.

Allosteric Activation of pThr 309-PKB by Hydrophobic Motif Peptides

To test the model that Ser 474 phosphorylation promotes an interaction between the hydrophobic motif and the induced hydrophobic groove of the N-terminal lobe, thereby causing an allosteric activation of the kinase, we assessed the ability of peptides modeled on the hydrophobic motif of PKB to activate the enzyme via an intermolecular association with the N-terminal lobe. First, we showed that toward Crosstide, a peptide substrate derived from the PKB phosphorylation site of

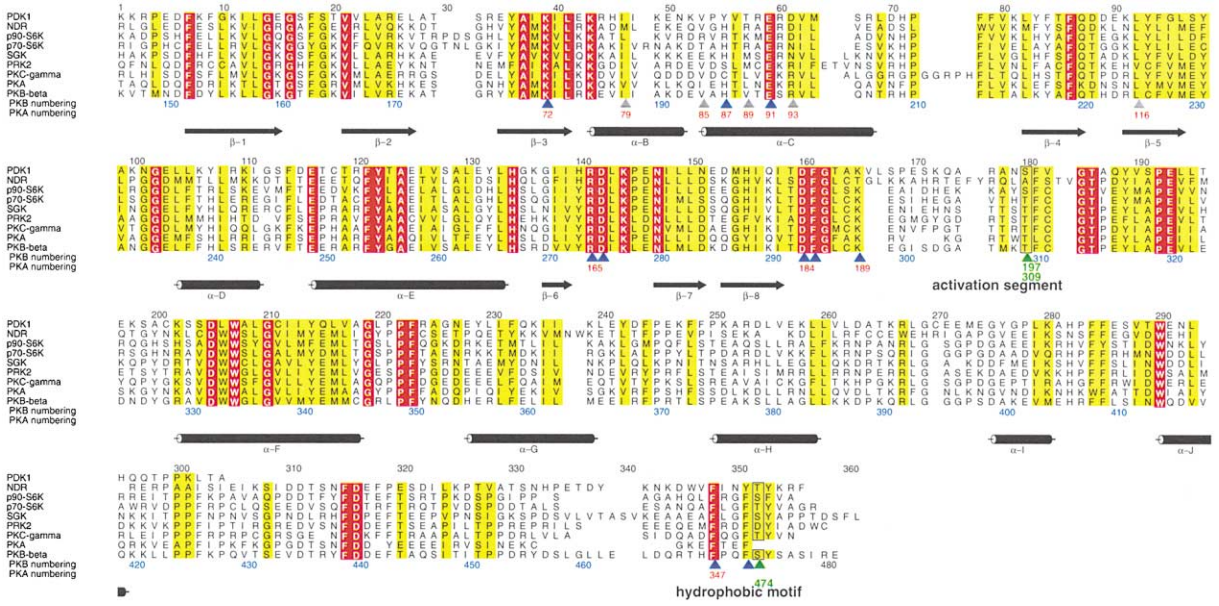

Figure 5. Multiple Sequence Alignment of Various AGC Kinases

Invariant residues are colored red, conserved are yellow. The positions of critical functional residues are indicated with a blue arrow and numbered according to PKA. PKB Thr 309 and Ser 474 phosphorylation sites are indicated. The conserved AGC kinase hydrophobic motif is shown and mutated residues of PKB that influence PIFtide activation (Figure 7B) are indicated by gray arrows. Figure drawn using ALSCRIPT (Barton, 1993).

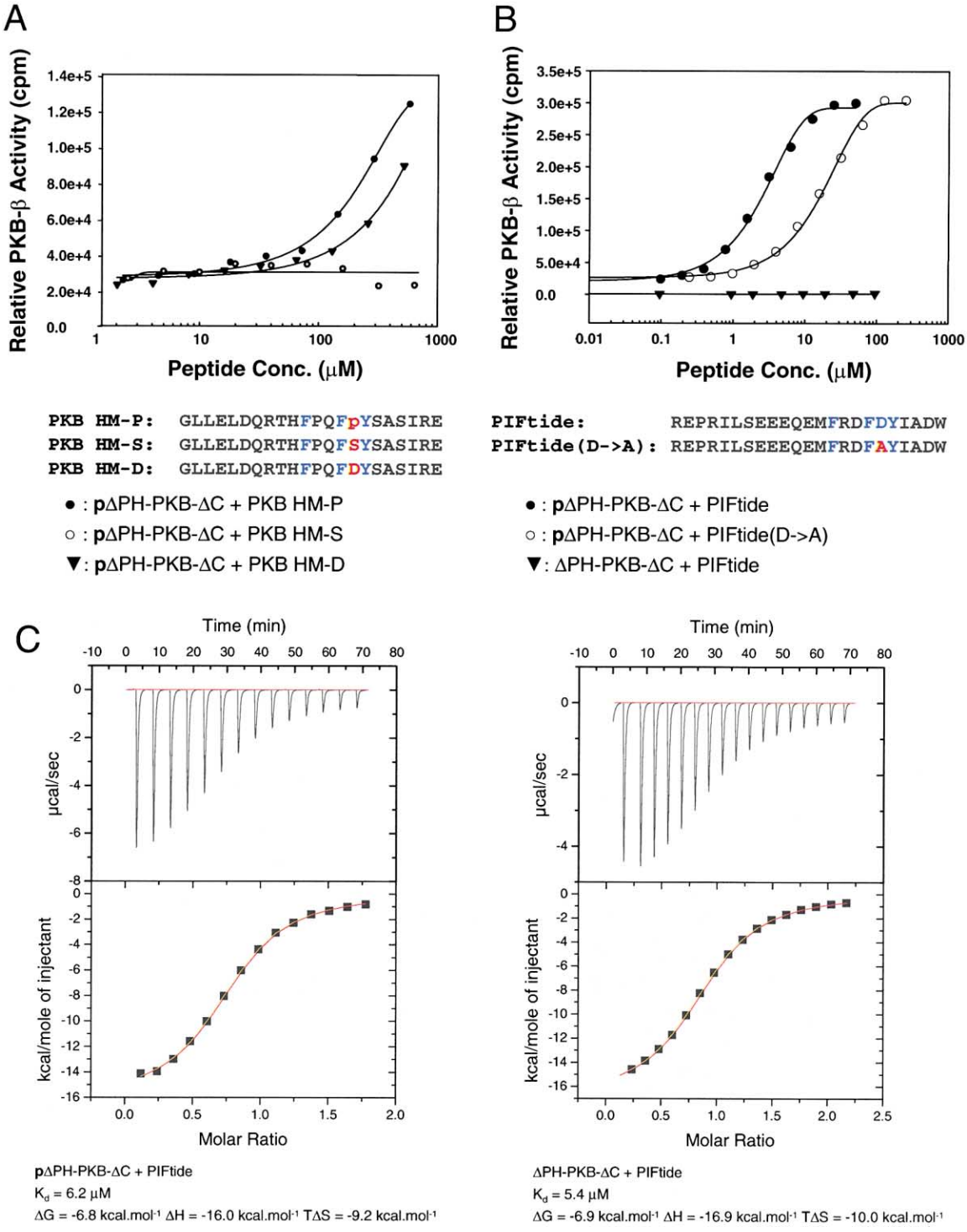

Figure 6. Activation of PKB by Hydrophobic Motif Peptide and PIFtide and Complex Formation between PKB and PIFtide

(A) Dose response curve for the stimulation of pΔPH-PKB-ΔC kinase activity by various PKB HM peptides, a synthetic 23 residue peptide encompassing the PKB HM motif. Closed circles, phosphorylated peptide; closed triangles, S474D mutant peptide; open circles, unphosphorylated peptide.

(B) Dose response curve for the stimulation of (p)ΔPH-PKB-ΔC kinase activity by PIFtide, a synthetic 24 residue peptide encompassing the PRK2 HM motif. Closed circles, PIFtide and pΔPH-PKB-ΔC; closed triangles, PIFtide and ΔPH-PKB-ΔC; open circles, mutant PIFtide(D>A) and pΔPH-PKB-ΔC. The maximal activity of PIFtide stimulated ΔPH-PKB-ΔC is 350 nmol/min/mg, equivalent to Thr 309 and Ser 474 phosphorylated ΔPH-PKB.

(C) Isothermal titration calorimetry measurements of the binding of PIFtide to pΔPH-PKB-ΔC (left) and ΔPH-PKB-ΔC (right). Upper panel, raw data of the titration of PIFtide into (p)ΔPH-PKB-ΔC. Lower panel, integrated heats of injections, corrected for the heat of dilution, with the solid line corresponding to the best fit of the data using the MicroCal software.

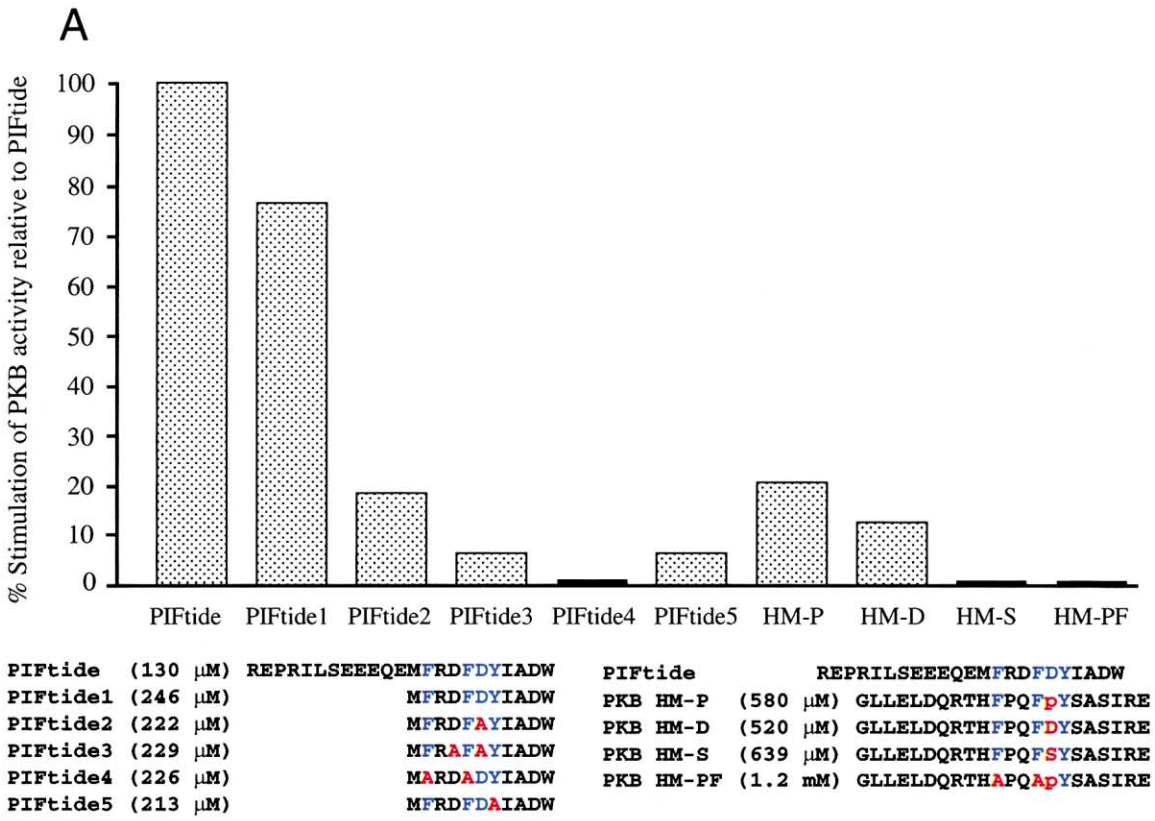

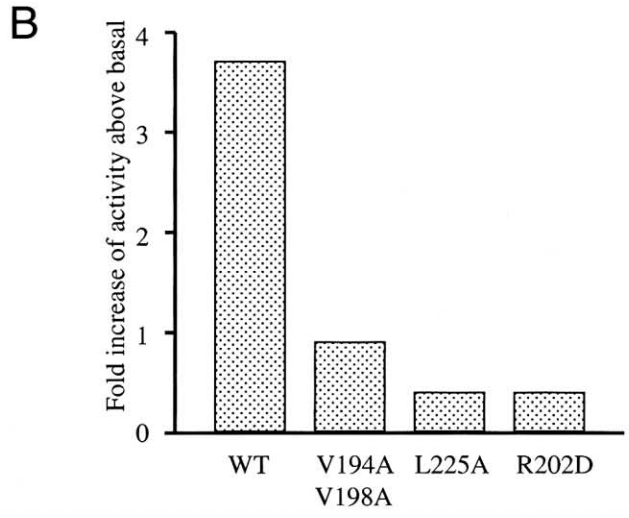

Figure 7. Conserved Residues of the Hydrophobic Motif, and Residues of the N Lobe of PKB, Are Required for PIFtide and PKB HM Peptide-Mediated Stimulation of PKB Kinase Activity

(A) Mutations of conserved hydrophobic motif residues of PIFtide and PKB HM peptide reduce or eliminate their potential to activate ΔPH-PKB-ΔC phosphorylated on Thr 309.

(B) Mutations of hydrophobic and electrostatic residues of the ΔPH-PKB-ΔC N lobe hydrophobic groove reduces the stimulation of PKB activity by 130 μM PIFtide. The positions of mutated residues on PKA and PKB (R202D, V194A-V198A, and L225A) are shown colored pink in Figures 2B and 2C and shown in Figure 5.

GSK-3, the unphosphorylated form of ΔPH-PKB-ΔC has no significant catalytic activity, whereas its Thr 309 phosphorylated counterpart was active. Addition of a peptide modeled on the phosphorylated hydrophobic motif of PKBβ (HM-P, residues 460-481) activated pΔPH-PKB-ΔC, with the stimulation reaching a maxi-

mum of 4-fold at 0.6 mM, the highest concentration of HM-P peptide achievable in our assay (Figure 6A). Significantly, this 4-fold stimulation of PKB by HM-P peptide is lower than the 7- to 10-fold stimulation of PKB by Ser 474 phosphorylation (Alessi et al., 1996). Analysis of the concentration-dependent activation of PKB by HM-P (Figure 6A) revealed that the binding sites for HM-P on ΔPH-PKB-ΔC were not fully titrated even at a peptide concentration of 0.6 mM, suggesting that higher concentrations of HM-P are necessary to fully stimulate PKB activity. The modest activation of PKB by HM-P peptide suggests a relatively low affinity of peptide for the PKB N-terminal lobe. An equivalent HM-peptide with an Asp substitution of Ser 474 was also capable of activating pΔPH-PKB-ΔC, consistent with studies showing that Asp mimics Ser 474 phosphorylation (Alessi et al., 1996). However, the maximum activation by this peptide was only 3-fold because of the lower affinity toward ΔPH-PKB-ΔC than the HM-P peptide (Figure 6A). Finally, as expected, the unphosphorylated HM peptide did not stimulate PKB activity.

Phosphorylation of a Ser or Thr residue within the hydrophobic motif is a conserved feature of the activation of varied AGC kinases, including PKC (Keranen et al., 1995) and the p70 and p90 S6 kinases (Pearson et al., 1995; Frodin et al., 2000). However, in some PKC isoforms, and in the PKC related kinase, PRK2, the site of Ser/Thr phosphorylation is replaced with either an Asp or Glu residue, suggesting that in these kinases, the hydrophobic motif will be constitutively activated, similarly to PKA, because of a permanent negative charge at this site. The C-terminal region of PRK2 that encompasses the carboxy-terminal hydrophobic motif was previously shown by Alessi and colleagues to interact tightly with the AGC kinase PDK1 (Balendran et al., 1999). PIFtide, a peptide representing the C-terminal 24 residues of PRK2, including its hydrophobic motif, was observed to stimulate PDK1 activity by 4-fold (Biondi et al., 2000). The findings of Biondi et al. (2000) prompted us to test whether PIFtide would also activate PKB by mimicking the HM-P peptide. Remarkably, we found that PIFtide activated pΔPH-PKB-ΔC by 15-fold, substantially more strongly than the activation achieved by the phosphorylated HM peptide. Analysis of the concentration dependence of pΔPH-PKB-ΔC activation by PIFtide revealed that the peptide binds the kinase with high affinity, resulting in a maximum and saturable activation at 20 μM and a corresponding EC_{50} value of 3 μM (Figure 6B). Significantly, the specific activity of pΔPH-PKB-ΔC maximally activated by PIFtide was 350 nmol/min/mg, essentially identical to the specific activity of ΔPH-PKB phosphorylated on both Thr 309 and Ser 474. Moreover, the latter form of PKB cannot be activated by PIFtide. PIFtide also promotes a 5-fold activation of ΔPH-PKB phosphorylated on Thr 309 to a specific activity similar to that of pΔPH-PKB-ΔC. The lower fold stimulation of ΔPH-PKB compared to that for pΔPH-PKB-ΔC can be explained by the partial phosphorylation of Ser-474 on pΔPH-PKB purified from *Sf*9 cells. Taken together, these data indicate that the stimulation of pΔPH-PKB-ΔC by an intermolecular association with PIFtide is equivalent to Ser 474 phosphorylation and the resultant intramolecular association between the N lobe of PKB and phosphorylated HM and furthermore suggests that an analysis of PKB-PIFtide interactions will provide insights concerning the mechanism of activation by Ser 474 phosphorylation.

Using isothermal titration calorimetry, we determined the affinity between PIFtide and both pΔPH-PKB-ΔC and ΔPH-PKB-ΔC (Figure 6C). First, we found that the equilibrium dissociation constant defining the interaction between PIFtide and pΔPH-PKB-ΔC was 6 μM, essentially identical to the EC_{50} value for the activation of pΔPH-PKB-ΔC by PIFtide (Figure 6B). This result suggests that the association of PIFtide to PKB correlates with the activation of the kinase. Second, we found that the interaction of PIFtide with pΔPH-PKB-ΔC is driven by a large negative enthalpy change (ΔH of –16.0 $kcal.mol^{-1}$) that compensates the energetically unfavorable decrease in entropy (TΔS of -9.2 $kcal.mol^{-1}$). The observed large decrease in entropy is not generally typical of protein-peptide interactions, for example SH2 domain-phosphotyrosine peptide complexes (Ladbury et al., 1995), and is consistent with an ordering of both the protein, presumably the αB and αC helices of the N lobe, and peptide on complex formation. Although PIFtide does not stimulate the activity of ΔPH-PKB-ΔC (Figure 6B), ITC data revealing a dissociation constant of 5.5 μM indicated that PIFtide interacts with this form of the enzyme as strongly as it does to phosphorylated ΔPH-PKB-ΔC, further emphasizing the crucial role of Thr 309 phosphorylation for PKB activity (Figure 6C) (Alessi et al., 1996).

The finding that PIFtide interacts with PKB with high affinity provided a model system for testing our notion that the essential role of Ser 474 phosphorylation is to promote the association of the hydrophobic motif with the N lobe of PKB. The residue of PIFtide equivalent to Ser 474 of PKB is an Asp, which presumably mimics a phosphorylated Ser 474 residue. To assess the importance of this residue for the ability of PIFtide to activate PKB, we determined the concentration-dependent activation of pΔPH-PKB-ΔC by PIFtide with an Ala residue substituting for the Asp. We found that, although higher concentrations of this mutant PIFtide(D→A) are required to activate pΔPH-PKB-ΔC than wild-type PIFtide, suggesting a lower affinity, the maximal activation of the kinase achieved by saturating concentrations of the mutant peptide is identical to that of the wild-type peptide (Figure 6B). The estimated EC_{50} value for PIFtide(D→A) is 20 μM, indicating an 8-fold lower affinity than PIFtide. ITC experiments also revealed an approximately 20-fold lower affinity between PIFtide(D→A) and pΔPH-PKB-ΔC relative to PIFtide. Thus, these experiments demonstrate an important concept that the PIFtide-induced conformational change of pΔPH-PKB-ΔC that results when PIFtide interacts with the kinase, and which leads to a maximal stimulation of the kinase activity, does not require a negatively charged residue at the equivalent of Ser 474 of the hydrophobic motif. The major role of a negative charge at this site is to increase the association of PIFtide with the PKB N lobe, whereas other residues, particularly the conserved Phe residues of the FxxF motif (see below), are more critical for promoting the conformational change responsible for activating the protein.

Because of the low affinity between pΔPH-PKB-ΔC and the PKB HM peptides, we were unable to determine

a K_D value defining their interaction with PKB using ITC. However, by assuming that the association between pΔPH-PKB-ΔC and the PKB HM peptides is an equilibrium process and that at saturating concentrations of peptide, the activation of pΔPH-PKB-ΔC will be similar to that induced by PIFtide, we used the data in Figure 6A and estimated the EC_{50} constants for the phosphorylated and S474D HM peptides to be 2.3 and 3.6 mM, respectively, an affinity ~1000-fold lower than for PIFtide.

Mutagenesis of the Hydrophobic Motif and N Lobe Hydrophobic Groove

By assessing the ability of modified PIFtide and HM peptides to activate pΔPH-PKB-ΔC, we delineated the role of conserved residues of the hydrophobic motif to induce the active conformation of PKB. For these experiments, we used an 11 residue peptide encompassing the 6 residue hydrophobic motif of PIFtide (PIFtide1, Figure 7A) that essentially recapitulates the activation of pΔPH-PKB-ΔC observed for the 23 residue PIFtide. The slightly lower activation suggests that residues of PIFtide N-terminal to the HM contribute to high-affinity PKB interactions. The PKB activities were determined at PIFtide concentrations ranging from 210–250 μM, where wild-type PIFtide fully activates PKB (Figures 6B and 7A). While all conserved residues of the HM motif contribute to PKB activation, significantly the two phenylalanine residues of the motif are essential for HM-induced activation. Ala substitutions of these residues in both PIFtide and the phosphorylated PKB HM peptide completely eliminated the potential of these peptides to stimulate PKB, even at PKB HM peptide concentrations of 1.2 mM (Figure 7A). A similar essential role for the equivalent Phe residues has been proposed for PKA where Ala substitutions lower the thermal stability and virtually abolish the catalytic activity of the enzyme (Etchebehere et al., 1997). Mutation of either the conserved Tyr residue or of both Asp residues of the PIFtide motif showed that these residues also contribute to the stimulatory affect of PIFtide on PKB activity (Figure 7A). PIFtide activates PKB by interacting with and simultaneously stabilizing the activated conformation of PKB. Therefore, the lower stimulatory effect of mutant PIFtide and PKB peptides most likely results from a reduced affinity for the activated conformation of PKB; however, because mutant PIFtide peptides have either low or no activity even at >200 μM, we were unable to determine EC_{50} values for their activation of PKB.

The crucial role of the conserved Phe residues of the hydrophobic motif to promote PIFtide and PKB HM peptide-mediated stimulation of PKB, and for the activity of PKA, suggests that they stabilize the active state of both PKB and PKA by a related structural mechanism. To test the notion that a hydrophobic groove is induced in PKB to engage the hydrophobic motif, and activate the kinase, we prepared a series of His tagged pΔPH-PKB-ΔC hydrophobic groove mutants and assessed their responsiveness to PIFtide. PKB mutants were transiently expressed in HEK cells, phosphorylated in vitro with PDK1, and purified using Ni-NTA agarose. SDS-PAGE and Western blot analysis of the purified fractions revealed that wild-type and mutant proteins were expressed to similar levels and that the enzyme was quantitatively isolated in a phosphorylated state. Moreover, the basal kinase activities of wild-type and mutant proteins were similar, indicating that the mutations did not disrupt the overall structure of the protein. Wild-type PKB prepared using this procedure was stimulated ~5-fold by 130 μM PIFtide (Figure 7B). The slightly lower activation probably results from incomplete Thr 309 phosphorylation, and consequently the PKB HM peptide did not elicit measurable activation. Replacing hydrophobic groove residues significantly reduced, but did not completely abolish, the potential of PIFtide to stimulate PKB (Figure 7B). Mutation of two αC helix residues, Val 194 and Val 198 (Ile 85 and Leu 89 of PKA), reduced PIFtide activation to only 25% of wild-type, whereas a Leu 225 mutant of the β-5 strand (Leu 116 of PKA) caused almost a complete loss of responsiveness to PIFtide (Figures 2, 5, and 7B).

Electrostatic interactions are important in defining high-affinity PIFtide and PKB HM peptide associations with PKB (Figure 6B) and form the basis for the increased affinity of the HM for the N lobe and subsequent activation of PKB by Ser 474 phosphorylation. Examination of the PKA and PKB crystal structures suggests that Arg 202 of the αC helix is likely to be important in mediating contacts to pSer 474 and the corresponding Asp residue of PIFtide. The equivalent residue of PKA, Arg 93, which is also conserved in PKC and PRK2, forms a water-mediated salt bridge to the carboxylate group of Glu 349 (Figures 2 and 4B). A charge reversal at this site (R202D) almost eliminates the ability of 130 μM PIFtide to activate PKB (Figure 7B), consistent with the notion that Arg 202 forms electrostatic contacts with PIFtide. However, analogous to our finding that at high concentrations, the PIFtide(D→A) mutant could activate PKB maximally (Figure 6B), the R202D PKB mutant was more responsive to higher concentrations of the peptide.

Discussion and Implications for Other AGC-Protein Kinases

This study presents a model for the regulation of PKB by hydrophobic motif phosphorylation. We describe data indicating that the role of HM phosphorylation is to induce an ordered N-terminal lobe as a result of an increased affinity between the hydrophobic motif and the hydrophobic groove. Ordering of the αC helix transmits a structural change to the activation segment and reorients the N and C lobes. We show that in the inactive PKB crystal structures residues of the αB and αC helices are disordered. Consistent with a disorder to order transition, the interaction of PIFtide with PKB is accompanied by a large negative entropy change. Mutation of key hydrophobic residues of the N lobe groove and hydrophobic motif either reduce or eliminate the ability of PIFtide to activate PKB. We showed by using PIFtide as a model system that the role of a negative charge within the HM (e.g., PKB Ser 474 phosphorylation) is to increase the affinity of the HM for the N lobe. In the context of the PKB kinase domain, phosphorylation of Ser 474 will increase the ability of the HM to interact with the N lobe via an intramolecular association. However, because we found that PIFtide(D→A) had only 8-fold lower affinity for PKB relative to PIFtide (Figure 6B), it

is likely that the unphosphorylated HM of PKB will still retain a weak affinity for the N lobe. We can therefore rationalize why PKB monophosphorylated on Thr 309 has between 7- to 10-fold lower activity than doubly phosphorylated PKB.

Disorder to order transitions of the αC helix as a result of phosphorylation represents a previously unrecognized mechanism for the stimulation of protein kinase activity. However, there is evidence that other AGC kinases undergo similar transitions, modulated by the hydrophobic motif. For example, phosphorylation of the HM of PKC increases its activity and resistance to temperature-induced denaturation (Bornancin and Parker, 1997) and the Phe residues of the PKA HM motif are critical for its stability and catalytic activity (Etchebehere et al., 1997). The conservation of the hydrophobic motif of AGC kinases is correlated with the invariance of the residues equivalent to Lys 76 and Leu 116 of PKA predicted to form the base of the hydrophobic groove in a number of diverse AGC kinases (Figures 4A and 5). Uniquely among AGC kinases, PDK1 lacks a C-terminal hydrophobic motif, although its N-terminal lobe hydrophobic groove is proposed to interact with PIFtide (Biondi et al., 2000). Similarly to our findings with PKB, high-affinity interactions between PIFtide and PDK1 required the conserved aromatic and Asp residues of the hydrophobic motif of the peptide (Balendran et al., 1999) and were disrupted by substitutions of PDK1 HM groove residues (Biondi et al., 2000).

The affinity of the HM-P peptide for PKB that is not phosphorylated on Ser 474 is ~1000-fold lower than that of PIFtide and is reminiscent of the low affinity of the tyrosine phosphorylated C terminus of Src for its own SH2 domain, compared with optimal phosphotyrosine binding sequences (Bradshaw et al., 1998). The covalent attachment of the phosphorylated hydrophobic motif to the PKB kinase domain will greatly increase its effective concentrations presumably in excess of the EC_{50} value estimated for the activation of PKB by the HM-P peptide. However, a modest mutual affinity may be important for two reasons. First, in order for phosphorylation of the HM to be capable of modulating its affinity for the N lobe, the affinity of the unphosphorylated HM for the N lobe must be sufficiently low to prevent the two from being constitutively associated. For example, a substitution of PIFtide(D→A) for the PKB HM motif would render PKB fully active and therefore unresponsive to HM phosphorylation. Second, it allows modulator proteins to gain access either to the hydrophobic groove or the phosphorylated motif, or for protein phosphatases to dephosphorylate pSer 474. Whether the activation of PKB by PIFtide reflects a biologically significant regulatory mechanism for stimulation of PKB by a modulator protein that interacts with the N lobe is unknown. However, the affinity of PIFtide for PKB may provide insight concerning the nature of the PDK2 enzyme responsible for phosphorylating Ser 474. A possible candidate for this enzyme is a kinase that interacts with the hydrophobic binding groove of PKB, perhaps via a sequence similar to the hydrophobic motif of PKB or PIFtide.

Experimental Procedures

Expression and Purification of ΔPH-PKB-ΔC and ΔPH-PKB

Generation of recombinant baculovirus using the GIBCO/Life Sciences Bacmid system was performed using standard procedures. *Sf*9 cells were lysed 72 hr post infection. The protein was purified using a combination of Q-sepharose anion exchange (Amersham), Ni-NTA (Qiagen), and phenyl TSK hydrophobic interaction (Tosohoas) chromatography, prior to removal of the N-terminal His tag by treatment with Tev protease. His tagged Tev protease was removed from cleaved PKB by Ni-NTA agarose. PKB was further purified using Q-sepharose anion exchange chromatography and by size exclusion using an S75 gel filtration column (Amersham). To prepare pΔPH-PKB-ΔC phosphorylated on Thr 309, the protein was incubated with PDK1 (purified from *Sf*9 cells) with 5 mM ATP/$MgCl_2$ for 2 hr at 20°C and for 14 hr at 4°C. Phosphorylated ΔPH-PKB-ΔC was separated from unphosphorylated ΔPH-PKB-ΔC by phenyl-TSK hydrophobic interaction chromatography and S75 gel filtration. ΔPH-PKB was purified in the same way as for ΔPH-PKB-ΔC, except that after the Ni-NTA purification, the enzyme was treated with λ protein phosphatase for 2 hr at 20°C to dephosphorylate the protein.

Crystallization of (p)ΔPH-PKB-ΔC and ΔPH-PKB

The protein was concentrated to 10 mg/ml and AMP-PNP/$MgCl_2$ was added to a final concentration of 5 mM. Crystals were grown using the under-oil batch method. 1 μl of protein was mixed with an equal volume of crystallization buffer: 30% (w/v) polyethylene glycol 4000, 0.2 M lithium sulfate, 0.1 M Tris.HCl (pH 8.5), and 5 mM DTT, within individual wells of a 72 well polystyrene tray, immersed under silicone oil, and incubated at 20°C.

Data Collection and Structure Determination

Crystals were incubated in a cryoprotection buffer comprising 18% (w/v) polyethylene glycol 4000, 120 mM lithium sulfate, 60 mM Tris.HCl (pH 8.5), 15% (v/v) polyethylene glycol 400, and 5 mM AMP-PNP/$MgCl_2$ for 20 s, prior to freezing in a nitrogen gas stream at 100 K. X-ray diffraction data were collected at ID14eh4, ESRF, Grenoble. Data were analyzed and processed using the HKL (Otwinowski and Minor, 1997) and CCP4 (1994) program suites. The structures of the three crystal forms of the PKB kinase domain were solved independently by means of molecular replacement using the coordinates of the catalytic subunit of mouse PKA (Knighton et al., 1991) with the program CNS (Brünger et al., 1998). The atomic structures were refined using rigid body and least squares refinement with CNS. Model building and analysis was done using O (Jones et al., 1991b).

Protein Kinase B Assay

PKB was assayed essentially as described by Andjelkovic et al. (1999) with 30 μM Crosstide (GRPRTSSAEG) as substrate without the PKA inhibitor peptide. For peptide stimulation experiments, the various peptides were added to the kinase assay mix prior to PKB. Peptides were synthesized by Franz Fischer at the FMI, Neosystem, France, and Severn Biotech, UK. The PKBβ HM peptide was GLLELDQRTH**FPQFS**^{474}**Y**SASIRE, with Ser 474 unphosphorylated, phosphorylated, and replaced with Asp, and the PIFtide sequence is REPRILSEEEQEM**FRDFDY**IADW. All experiments were performed in either duplicate or triplicate.

Isothermal Titration Calorimetry

Isothermal titration calorimetry (ITC) was performed using a MCS ITC (MicroCal). All protein and peptide samples were previously dialysed into a buffer comprising 75 mM Tris.HCl (pH 8.0), 100 mM NaCl, and 5 mM DTT. Titrations were performed by injecting 15–20 consecutive aliquots (15 μl) of peptide solution (0.7–1.5 M) into the ITC cell containing PKB (70–170 μM) at 14°C. ITC data were corrected for heat of dilution of PKB solutions. Binding stoichiometry, enthalpy, and equilibrium association constants were determined by fitting corrected data to a bimolecular interaction model.

Mapping and Quantification of the Phosphorylation Sites by Mass Spectrometry

The SDS-PAGE separated proteins were excised from the gel, reduced with DDT, alkylated with iodoacetamide, cleaved with trypsin (Promega, sequencing grade), and extracted from the gel as described by Shevchenko et al. (1996). Peptides were fractionated and analyzed by LC-MS. The potential phosphopeptides were identified in the LC fraction by mass and further analyzed by NanoESI MSMS to confirm the sequence and phosphorylation site within the peptides according to the method of Wilm & Mann (1996). Approximate quan-

tification was done by extraction and integration of the ions of interest for the phosphorylated as well as the nonphosphorylated form of the peptides in the corresponding LC-MS runs.

Expression in HEK293 Cells and Purification of PKB and Mutants

pFastBacHTaΔPHPKBβΔC (residues 146-460) expression vector was used as template for mutagenesis by the Quik Change (Stratagene) method. The His-tagged cDNAs encoding the wild-type and mutant derivatives were transferred from the pFastBacHTA plasmid to pcDNA3.1 (Hygromycin). pcDNA3.1.ΔPHPKBβΔC wild-type and mutant derivatives were transfected into HEK293 cells (Hill and Hemmings, 2002). For purification of PKB, fifty 10 cm tissue culture plates were transfected with 10 μg DNA per plate with the appropriate construct of 48 or 72 hr in DMEM medium containing 10% serum at 37°C.

Cells were harvested by washing with ice-cold phosphate buffered saline and lysed into PKB lysis buffer (50 mM Tris-HCl [pH 7.5] containing 25 mM NaF, 40 mM β-glycerophosphate, 120 mM NaCl, 1% NP-40, 0.1 μM sodium vanadate, 2 μM microcystin, l μM benzamidine, and 1 μM PMSF). Lysates were snap frozen in liquid nitrogen and stored at –80°C prior to use. Frozen lyzates from 50 plates were thawed and centrifuged prior to loading onto 1 ml (packed volume) of Ni-NTA (Qiagen) resin equilibrated in PBS buffer. The Ni-NTA resin was extensively washed with PBS followed by 50 mM Tris-Cl (pH 7.4) and 0.5 mM EDTA.

To phosphorylate ΔPHPKBβΔC, the kinase isolated using Ni-NTA resin was treated with PDK1 (100 μg), 5 mM MgAcetate, and 5 mM ATP, in 50 mM Tris-Cl (pH 7.4) in a total volume of 1 ml for 3 hr at 22°C followed by incubation at 4°C for 12 hr. The resin was then washed with PBS followed by 50 mM Tris-HCl (pH 7.5) and 0.5 mM EDTA. PKBβ was eluted using 80 mM Tris-HCl (pH 7.9), 0.5 M imidazole, and 0.5 M NaCl.

Acknowledgments

We thank the staff at the ESRF, Grenoble, for access to synchrotron radiation facilities. The work was supported by grants from the Cancer Research UK, BBSRC, and ICR to D.B. We thank the following for invaluable help: Angela Paul (mass. spec. analysis), Maceiej Pietrzak (DNA sequencing), and Franz Fischer (peptide synthesis) and Ronan O'Brien and Peter Oliver of MicroCal, LCC, for the ITC. The FMI is part of the Novartis Research Foundation.

Received December 4, 2001
Revised March 27, 2002

References

Alessi, D.R., Andjelkovic, M., Caudwell, B., Cron, P., Morrice, N., Cohen, P., and Hemmings, B.A. (1996). Mechanism of activation of protein kinase B by insulin and IGF-1. EMBO J. *15*, 6541–6551.

Alessi, D.R., James, S.R., Downes, C.P., Holmes, A.B., Gaffney, P.R., Reese, C.B., and Cohen, P. (1997). Characterization of a 3-phosphoinositide-dependent protein kinase which phosphorylates and activates protein kinase Bα. Curr. Biol. *7*, 261–269.

Andjelkovic, M., Maira, S.M., Cron, P., Parker, P.J., and Hemmings, B.A. (1999). Domain swapping used to investigate the mechanism of protein kinase B regulation by 3-phosphoinositide-dependent protein kinase 1 and Ser473 kinase. Mol. Cell. Biol. *19*, 5061–5072.

Balendran, A., Casamayor, A., Deak, M., Paterson, A., Gaffney, P., Currie, R., Downes, C.P., and Alessi, D.R. (1999). PDK1 acquires PDK2 activity in the presence of a synthetic peptide derived from the carboxyl terminus of PRK2. Curr. Biol. *9*, 393–404.

Barton, G.J. (1993). ALSCRIPT: a tool to format multiple sequence alignments. Protein Eng. *6*, 37–40.

Bellacosa, A., Testa, J.R., Staal, S.P., and Tsichlis, P.N. (1991). A retroviral oncogene, akt, encoding a serine-threonine kinase containing an SH2-like region. Science *254*, 274–277.

Biondi, R.M., Cheung, P.C., Casamayor, A., Deak, M., Currie, R.A., and Alessi, D.R. (2000). Identification of a pocket in the PDK1 kinase domain that interacts with PIF and the C-terminal residues of PKA. EMBO J. *19*, 979–988.

Bornancin, F., and Parker, P.J. (1997). Phosphorylation of protein kinase Cα on serine 657 controls the accumulation of active enzyme and contributes to its phosphatase-resistant state. J. Biol. Chem. *272*, 3544–3549.

Bradshaw, J.M., Grucza, R.A., Ladbury, J.E., and Waksman, G. (1998). Probing the "two-pronged plug two-holed socket" model for the mechanism of binding of the Src SH2 domain to phosphotyrosyl peptides: a thermodynamic study. Biochemistry *37*, 9083–9090.

Brazil, D.P., and Hemmings, B.A. (2001). Ten years of protein kinase B signalling: a hard Akt to follow. Trends Biochem. Sci. *26*, 657–664.

Brodbeck, D., Hill, M.M., and Hemmings, B.A. (2001). Two splice variants of protein kinase B gamma have different regulatory capacity depending on the presence or absence of the regulatory phosphorylation site serine 472 in the carboxyl-terminal hydrophobic domain. J. Biol. Chem. *276*, 29550–29558.

Brünger, A.T., Adams, P.D., Clore, G.M., DeLano, W.L., Gros, P., Grosse-Kunstleve, R.W., Jiang, J.S., Kuszewski, J., Nilges, M., Pannu, N.S., et al. (1998). Crystallography and NMR system: a new software suite for macromolecular structure determination. Acta Crystallogr. D Biol. Crystallogr. *54*, 905–921.

Cantley, L.C., and Neel, B.G. (1999). New insights into tumor suppression: PTEN suppresses tumor formation by restraining the phosphoinositide 3-kinase/AKT pathway. Proc. Natl. Acad. Sci. USA *96*, 4240–4245.

CCP4 (Collaborative Computational Project 4) (1994). The CCP4 suite: programs for protein crystallography. Acta Cryst. D *50*, 760–763.

Coffer, P.J., and Woodgett, J.R. (1991). Molecular cloning and characterisation of a novel putative protein-serine kinase related to the cAMP-dependent and protein kinase C. Eur. J. Biochem. *201*, 475–481.

Datta, S.R., Brunet, A., and Greenberg, M.E. (1999). Cellular survival: a play in three Akts. Genes Dev. *13*, 2905–2927.

Esnouf, R.M. (1997). An extensively modified version of MOLSCRIPT that includes greatly enhanced coloring capabilities. J. Mol. Graph. Model. *15*, 132–134.

Etchebehere, L.C., Van Bemmelen, M.X., Anjard, C., Traincard, F., Assemat, K., Reymond, C., and Veron, M. (1997). The catalytic subunit of Dictyostelium cAMP-dependent protein kinase—role of the N-terminal domain and of the C-terminal residues in catalytic activity and stability. Eur. J. Biochem. *248*, 820–826.

Frodin, M., Jensen, C.J., Merienne, K., and Gammeltoft, S. (2000). A phosphoserine-regulated docking site in the protein kinase RSK2 that recruits and activates PDK1. EMBO J. *19*, 2924–2934.

Hill, M.M., and Hemmings, B.A. (2002). Analysis of protein kinase B/Akt. Methods Enzymol. *345*, 448–463.

Hubbard, S.R., Wei, L., Ellis, L., and Hendrickson, W.A. (1994). Crystal structure of the tyrosine kinase domain of the human insulin receptor. Nature *372*, 746–754.

Johnson, L.N., Noble, M.E., and Owen, D.J. (1996). Active and inactive protein kinases: structural basis for regulation. Cell *85*, 149–158.

Jones, P.F., Jakubowicz, T., Pitossi, F.J., Maurer, F., and Hemmings, B.A. (1991a). Molecular cloning and identification of a serine/threonine protein kinase of the second-messenger subfamily. Proc. Natl. Acad. Sci. USA *88*, 4171–4175.

Jones, T.A., Zou, J.Y., Cowan, S.W., and Kjeldgaard, M. (1991b). Acta Crystallogr. A *50*, 157–160.

Keranen, L.M., Dutil, E.M., and Newton, A.C. (1995). Protein kinase C is regulated in vivo by three functionally distinct phosphorylations. Curr. Biol. *5*, 1394–1403.

Knighton, D.R., Zheng, J.H., Ten Eyck, L.F., Xuong, N.H., Taylor, S.S., and Sowadski, J.M. (1991). Structure of a peptide inhibitor bound to the catalytic subunit of cyclic adenosine monophosphate-dependent protein kinase. Science *253*, 414–420.

Ladbury, J.E., Lemmon, M.A., Zhou, M., Green, J., Botfield, M.C., and Schlessinger, J. (1995). Measurement of the binding of tyrosyl phosphopeptides to SH2 domains: a reappraisal. Proc. Natl. Acad. Sci. USA *92*, 3199–3203.

Maira, S.M., Galetic, I., Brazil, D.P., Kaech, S., Ingley, E., Thelen, M., and Hemmings, B.A. (2001). Carboxyl-terminal modulator protein

(CTMP), a negative regulator of PKB/Akt and v-Akt at the plasma membrane. Science *294*, 374–380.

Mayo, L.D., and Donner, D.B. (2001). A phosphatidylinositol 3-kinase/Akt pathway promotes translocation of Mdm2 from the cytoplasm to the nucleus. Proc. Natl. Acad. Sci. USA *98*, 11598–11603.

Merit, E.A., and Murphy, M.E.P. (1994). Raster3D Version 2.0. A program for photorealistic molecular graphics. Acta Crystrallogr. D. *50*, 869–873.

Nicholls, A., Sharp, K.A., and Honig, B. (1991). Protein folding and association: insights from the interfacial and thermodynamic properties of hydrocarbons. Proteins *11*, 281–296.

Otwinowski, Z., and Minor, W. (1997). Processing of x-ray diffraction data collected in oscillation mode. Methods Enzymol. *276*, 307–326.

Pearson, R.B., Dennis, P.B., Han, J.W., Williamson, N.A., Kozma, S.C., Wettenhall, R.E., and Thomas, G. (1995). The principal target of rapamycin-induced p70s6k inactivation is a novel phosphorylation site within a conserved hydrophobic domain. EMBO J. *14*, 5279–5287.

Shevchenko, A., Wilm, M., Vorm, O., and Mann, M. (1996). Mass spectrometric sequencing of proteins silver-stained polyacrylamide gel. Anal. Chem. *68*, 850–858.

Shoji, S., Titani, K., Demaille, J.G., and Fischer, E.H. (1979). Sequence of two phosphorylated sites in the catalytic subunit of bovine cardiac muscle adenosine 3′:5′-monophosphate-dependent protein kinase. J. Biol. Chem. *254*, 6211–6214.

Staal, S.P., Hartley, J.W., and Rowe, W.P. (1977). Isolation of transforming murine leukemia viruses from mice with a high incidence of spontaneous lymphoma. Proc. Natl. Acad. Sci. USA *74*, 3065–3067.

Stephens, L., Anderson, K., Stokoe, D., Erdjument-Bromage, H., Painter, G.F., Holmes, A.B., Gaffney, P.R., Reese, C.B., McCormick, F., Tempst, P., et al. (1998). Protein kinase B kinases that mediate phosphatidylinositol 3,4,5-trisphosphate-dependent activation of protein kinase B. Science *279*, 710–714.

Stokoe, D., Stephens, L.R., Copeland, T., Gaffney, P.R., Reese, C.B., Painter, G.F., Holmes, A.B., McCormick, F., and Hawkins, P.T. (1997). Dual role of phosphatidylinositol-3,4,5-trisphosphate in the activation of protein kinase B. Science *277*, 567–570.

Testa, R., and Bellacosa, A. (2001). AKT plays a central role in tumorigenesis. Proc. Natl. Acad. Sci. USA *98*, 10983–10985.

Vanhaesebroeck, B., and Alessi, D.R. (2000). The PI3K-PDK1 connection: more than just a road to PKB. Biochem. J. *346*, 561–576.

Williams, M.R., Arthur, J.S., Balendran, A., van der Kaay, J., Poli, V., Cohen, P., and Alessi, D.R. (2000). The role of 3-phosphoinositide-dependent protein kinase 1 in activating AGC kinases defined in embryonic stem cells. Curr. Biol. *10*, 439–448.

Wilm, M., and Mann, M. (1996). Analytical properties of the nanoelectrospray ion source. Anal. Chem. *68*, 1–8.

Yonemoto, W., McGlone, M.L., Grant, B., and Taylor, S.S. (1997). Autophosphorylation of the catalytic subunit of cAMP-dependent protein kinase in Escherichia coli. Protein Eng. *10*, 915–925.

Accession Numbers

Protein coordinates have been deposited with ID accession codes 1GZK (pΔPH-PKB-ΔC), 1GZO (ΔPH-PKB-ΔC), and 1GZN (ΔPH-PKB).